P-96: Analysis of Address Discharge Delay Characteristics Using Transient Characteristics of IR Emission Intensity in Plasma Display Panel

Hyung Dal Park, Jae Hyun Kim, and Heung-Sik Tae
School of Electronics Engineering, College of IT Engineering, Kyungpook National University, Daegu, South Korea

Deok Myeong Kim and Jeong Hyun Seo
Dept. of Electronics Engineering, Univ. of Incheon, Incheon, South Korea

Abstract
This paper analyzes the address discharge delay characteristics based on the measurement of the transient IR emission intensity according to the wall charge state after the reset discharge. This measurement result shows that the maximal erasure of the wall charges accumulating on the scan and address electrodes during the negative ramp-falling period induces the easy transition from the weak discharge to the strong discharge, thereby resulting in shortening the statistical delay time.

1. Introduction
In the current driving of AC-PDP, to express the image with the various gray levels, ADS (Address Display Separated) driving scheme that uses over 8 subfields has been employed. Each subfield is consisted with the reset-, address-, and sustain-periods. To improvement of an image quality in AC-PDPs, full high definition (HD) PDP requires a wider driving margin and more stable address discharge. Especially, the stable address discharge under a high speed address procedure strongly depends on the wall charge states accumulating among the three electrodes prior to an initiation of address discharge [1]-[3]. In this sense, the discharge characteristics of various wall charges states prior to the address discharge need to be investigated intensively. The weak and strong discharge regions of the XY-AY simultaneous discharge region are very important for address discharge after reset discharge, especially [2]. Accordingly, this paper analyzes the transient characteristics of IR emission intensity in the XY-AY simultaneous discharge region and compares the address discharge characteristics by the wall charge states after reset discharge using the address discharge delay time.

2. Experimental Setup
Fig. 1 shows the test panel used in this work was commercial 50-in. full HD AC-PDP with a box-type barrier rib. The gas mixture and pressure of test panel were Ne-He-Xe (11%) and 420 Torr, respectively.

Fig. 2 shows the schematic diagram of experimental setup employed in this study. As shown in Fig. 2, the IR emission (823 nm) Intensity measurement systems and the 50-in. full-HD test panel with three electrodes used in the experiments, where X is the common electrode, Y is scan electrode, and A is the address electrode. A PMT

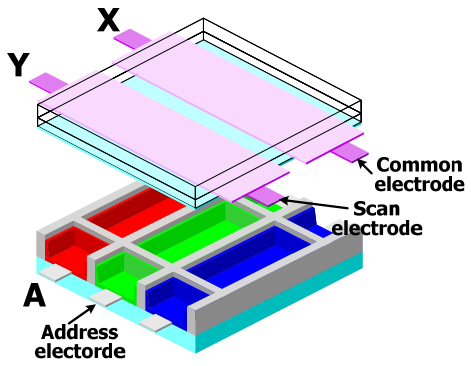

Fig. 1. Commercial 50-in. full HD AC-PDP with a box-type barrier rib used in this work.

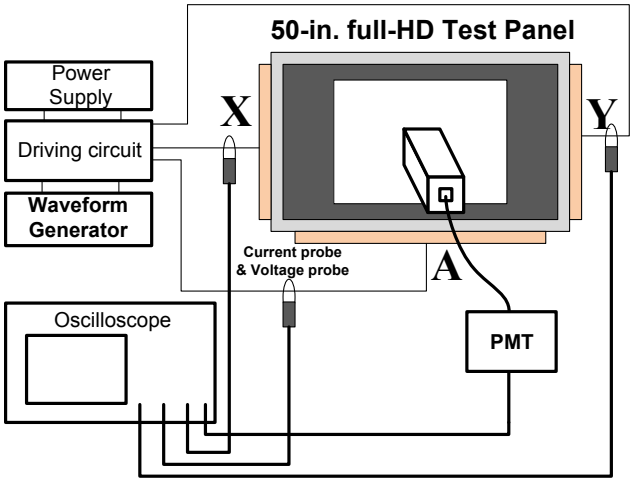

Fig. 2. Schematic diagram of experimental setup employed in this study for measuring IR (823 nm) transient characteristics and address discharge delay time in test panel.

(photomultiplier tube) and the waveform generator were used to measure the IR emission intensity and address discharge delay time after the various reset discharge.

Fig. 3 shows the driving waveform for measuring the transient characteristics of IR emission intensity after reset discharge. The conventional reset waveforms of three cases among the three electrodes were applied to produce the reset discharge. In addition, to exclude the priming effect,

 ISSN 0097-966X/11/4203-1468-$1.00

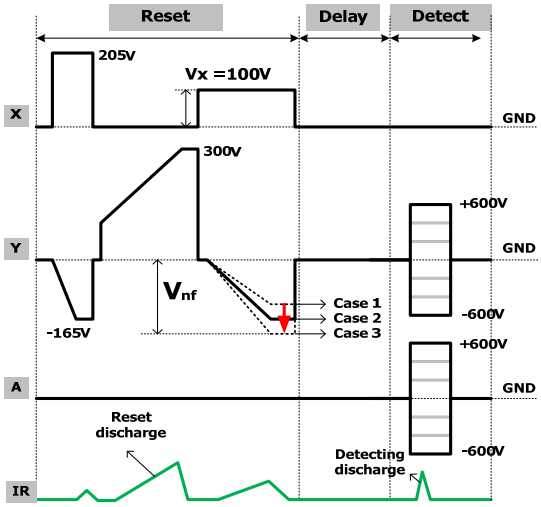

Fig. 3. Schematic diagrams of driving waveform for measuring the transient characteristics of IR emission intensity after reset discharge.

Table 1. Various voltages used in case study and voltage levels.

Cases	Vnf	Vscanl
Case 1	-145 V	-165 V
Case 2	-175 V	-195 V
Case 3	-205 V	-225 V

Voltage level

Vs	205 V	Vx	100 V	Va	55 V

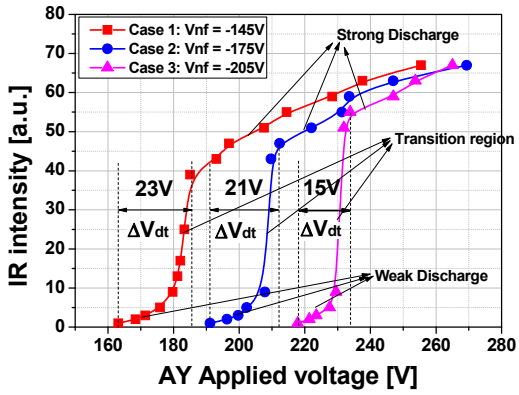

Fig. 4. Measured transient characteristics of IR emission intensity after reset discharge in XY-AY simultaneous discharge region.

the detecting pulse was applied after 200 μs. The IR emission intensities are measured by increasing the applied voltage of detecting pulse during detect-period. Where the

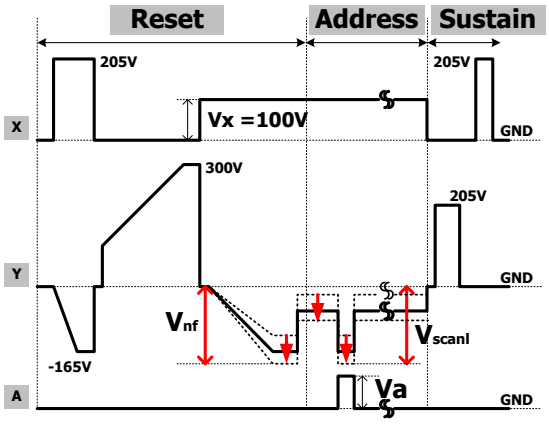

Fig. 5. Schematic diagrams of the driving waveforms employed in the current study.

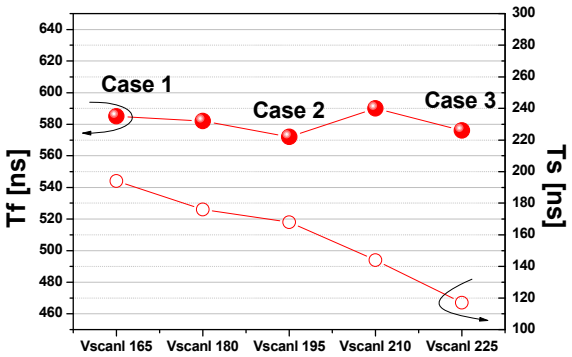

Fig. 6. Address discharge delay time by the driving waveforms of various cases.

negative falling-ramp voltage levels (Vnf) are decreased to the three voltage levels: -145 V (case 1), -175V (case2), and -205V (case 3), respectively. The detailed voltage levels are listed in Table 1. In the case 3, the accumulated wall charges between scan and address electrodes are more erased than the cases 1 and 2 during the negative falling-ramp period.

3. Results

3.1. Transient Characteristics of IR Emission Intensity after Reset Discharge

Fig. 4 shows the measured transient characteristics of IR emission intensity after the reset discharge of various cases in the XY-AY simultaneous discharge region. As shown in Fig. 4, the IR emission intensities are separated by the three regions such as weak discharge, transition region, and strong discharge. In the case 1, the IR intensity is slowly increased by increasing the applied voltage from weak

discharge to strong discharge. And the voltage difference of transition (ΔVdt) from the weak discharge to the strong discharge is about 23 V. On the other hand, in the cases 2 and 3, the IR intensity is sharply increased by increasing the applied voltage from the weak discharge to the strong discharge. The voltage differences of transitions (ΔVdt) from the weak discharge to the strong discharge are about 21 V and 15V, respectively. Especially, as shown in the case 3 of Fig. 4, it is observed that the IR emission intensity is dramatically increased and easily generated the strong IR emission by the small A-Y voltage difference of transition (ΔVdt). It means that the large erasure of the wall charges accumulating on the scan and address electrodes during the negative falling-ramp period induces the easy transition from the weak discharge to the strong discharge. Furthermore, the strong discharge is generated. Accordingly, this analyzed results show that the transient characteristics of IR emission intensity are changed by the wall charge states from the weak discharge to the strong discharge.

3.2. Address Discharge Characteristics after Reset Discharge

Fig. 5 shows the schematic diagrams of the driving waveforms for measuring the address discharge delay time relative to the wall charge states of three cases. The detailed voltage levels of each cases is listed Table 1.

Fig. 6 shows the address discharge delay time by the driving waveforms of various cases. As shown in Fig. 6, in the case 3, the statistical delay time (Ts) are reduced by about 80 ns causing the strong IR emission intensity is generated by the easy transition from the weak discharge to the strong discharge. However, the formative delay time (Tf) is almost same causing the same cell voltages (Vcell=Vwall+Vapplied) by the driving waveforms of three cases.

4. Conclusions

This paper analyzes the address discharge delay characteristics based on the measurement of the transient IR emission intensity according to the wall charge state after the reset discharge. This measurement result shows that the maximal erasure of the wall charges accumulating on the scan and address electrodes during the negative ramp-falling period induces the easy transition from the weak discharge to the strong discharge, thereby resulting in shortening the statistical delay time.

5. References

[1] B. J. Shin, “Characteristics of an address discharge time lag in terms of a wall voltage in an AC PDP,” IEEE Transactions on Electron Devices, vol.53, no.7, 1539-1542,(2006).

[2] K. Sakita, K. Takayama, K. Awamoto, and Y. Hashimoto, “High-speed address driving waveform analysis using wall voltage transfer function for three terminals and Vt close curve in three-electrode surface-discharge AC-PDPs,” SID’01 Digest, 1022-1025, (2001).

[3] H. D. Park, J. Y. Kim, and H.-S. Tae, "Analysis of statistical time lags based on wall charges prior to address discharge using Vt close-curve method for full-HD AC-PDP," SID’07 Digest, 569-572, (2007).